analytical chemistry

Article

pubs.acs.org/ac

Near-Infrared Fluorescence Probe for Monitoring the Metabolic Products of Vitamin C in HepG2 Cells under Normoxia and Hypoxia

Xiaohong Pan,[†,‡] Xiaoting Wang,[†] Liyong Wang,[†] Kehua Xu,*[,†] Fanpeng Kong,[†] and Bo Tang*[,†]

[†]Collaborative Innovation Center of Functionalized Probes for Chemical Imaging in Universities of Shandong, Key Laboratory of Molecular and Nano Probes, Ministry of Education, Shandong Provincial Key Laboratory of Clean Production of Fine Chemicals, College of Chemistry, Chemical Engineering and Materials Science, Shandong Normal University, Jinan 250014, People's Republic of China

[‡]Department of Pharmaceutical Sciences, Binzhou Medical University, Shandong Yantai 264003, People's Republic of China

Supporting Information

ABSTRACT: Vitamin C (ascorbic acid; AA) is a well-known reducing agent and has been evaluated for its antitumor activity. However, the mechanism for its antitumor action remains unclear. Tracking the metabolism of AA may help to elucidate its antitumor mechanism. In this study, a near-infrared fluorescent probe (Arg-Cy) for monitoring the metabolic products of AA in living cells was developed based on the reaction of the guanidine group in Arg-Cy with the adjacent diketone involved in the metabolites of AA. Consequently, the probe can respond to L-xylosone, a metabolite of AA, with high selectivity and sensitivity and was successfully used to visualize the real-time changes of L-xylosone levels in living cells incubated under normoxic conditions. Considering that the tumor microenvironment suffers from hypoxia, the L-xylosone levels in the process of HepG2 cell death induced by pharmacological doses of AA were also monitored under hypoxic conditions. Surprisingly, no obvious fluorescence change appeared during this process. Furthermore, detection of the intracellular redox state using a reported H_2O_2 probe confirmed that AA can be metabolized to L-xylosone only under normoxic conditions due to the oxidative stress, but not under hypoxic conditions. Therefore, we hypothesize that the mechanism for cell death induced by AA under hypoxia is different from that under normoxia. Thus, the developed probe can provide a tool for monitoring the metabolism of AA and may help to clarify the mechanism for the antitumor activity of vitamin C in the tumor microenvironment.

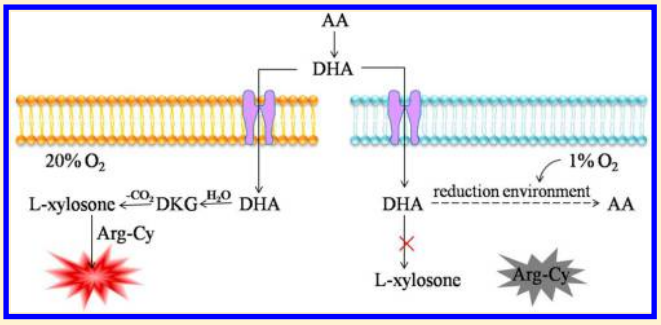

Vitamin C (Vc), which is available in reduced form (ascorbic acid; AA) and in oxidized form (dehydroascorbic acid; DHA), is often used in health care supplements as an antioxidant.[1,2] In recent years, because of their low systemic toxicity, AA and DHA have been evaluated for their antitumor activities.[3,4] In previous studies, cells cultured under normoxic conditions were used to investigate the cytotoxic effects of pharmacological doses of AA/DHA on tumor cells. The research results demonstrated that vitamin C can act as a prooxidant molecule promoting the formation of reactive oxygen species (ROS) and resulting in oxidative stress which triggers cell apoptosis.[5,6] However, it is well-known that vitamin C is a reducing agent (antioxidant) that can neutralize free radicals and decrease oxidative stress[7,8] and that the tumor microenvironment suffers from hypoxia (low levels of O_2) because newly developing blood vessels are aberrant and have poor blood flow.[9,10] Thus, this conflict is puzzling. Developing a method for imaging the metabolic products of vitamin C may help to clarify this question.

At present, only a few studies have investigated the metabolic products of vitamin C. In 1996, Pischetsrieder found that L-xylosone is a main metabolic product of vitamin C based on high-performance liquid chromatography (HPLC) and UV spectra.[11] Simpson and Ortwerth determined that L-erythrulose and oxalate are the primary degradation products of AA under physiological conditions based on proton-decoupled ^{13}C nuclear magnetic resonance spectroscopy (^{13}C NMR) and quantified these degradation products using HPLC.[12] Nemet and Monnier found five degradation products, including dehydroascorbic acid, 2,3-diketogulonic acid, 3-deoxythreosone, L-xylosone, and threosone, in the human lens using liquid chromatography/mass spectrometry (LC/MS).[13] However, the before-mentioned methods cannot realize the real-time observation of the metabolic products of vitamin C in living cells and in vivo. To better clarify the antitumor mechanism of vitamin C, it is necessary to develop a dynamic visualization analysis method for Vc metabolites in vivo. Fluorescence detection is recognized to possess both high sensitivity and high spatiotemporal resolution for the real-time visualization of biomolecules in vitro and in vivo.[14,15] However, no fluorescence

Received: March 2, 2015
Accepted: June 18, 2015
Published: June 18, 2015

DOI: 10.1021/acs.analchem.5b00820
Anal. Chem. 2015, 87, 7092−7097

Scheme 1. Synthesis of Arg-Cy and Its Response Mechanism to L-Xylosone

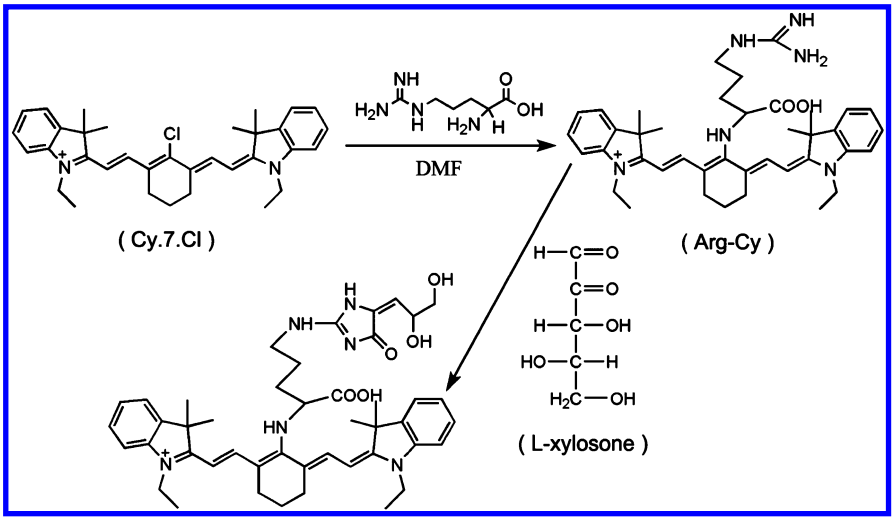

probes have been developed for imaging the metabolic process of vitamin C.

In this report, a near-infrared (NIR) fluorescence probe (Arg-Cy) was designed and synthesized by conjugating L-arginine to tricarbochlorocyanine dye (Cy.7.Cl) for monitoring the metabolic products of vitamin C in cancer cells. The developed probe can be used to specifically detect L-xylosone, one of the metabolites of AA, based on the reaction between the guanidine residue of Arg-Cy and the adjacent diketone group of L-xylosone (Scheme 1). This probe was successfully used to image the L-xylosone levels in living cells when HepG2 cells were treated with pharmacological doses of AA under both normoxic conditions and hypoxic conditions. Under normoxia, increased L-xylosone levels were detected in the process of cell death induced by AA, which were accompanied by a higher H_2O_2 level. In contrast, no detectable fluorescence enhancement was observed under hypoxia, and the change in the H_2O_2 level was negligible. These results indicate that, under hypoxia, AA cannot be metabolized to L-xylosone and that no oxidative stress occurs in the process of cell death.

EXPERIMENTAL SECTION

Materials and Methods. Ascorbic acid, dehydroascorbic acid, L-arginine, and xanthine/xanthine oxidase (X/XO) were purchased from Sigma-Aldrich. Sodium nitroferricyanide(III) dihydrate (SNP) was purchased from Alfa Aesar (Tianjin, China). All other chemicals and solvents used were local products of analytical grades. 2-[4-Chloro-7-(1-ethyl-3,3-dimethyl(indolin-2-ylidene)]-3,5-(propane-1,3-diyl)-1,3,5-heptatrien-1-yl)-1-ethyl-3,3-dimethyl-3*H*-indolium (Cy.7.Cl) was synthesized in our laboratory.[16] A stock solution (1 mM) of Arg-Cy was prepared by dissolving in dimethyl sulfoxide (DMSO). Ultrapure water (18.2 MΩ cm) was used throughout the analytical experiments. HepG2 cells were purchased from the Committee on Type Culture Collection of the Chinese Academy of Sciences. ^{1}H NMR spectrum was taken on a nuclear magnetic resonance spectrometer (AVANCE 300, Bruker, Switzerland). Electrospray ionization mass spectra (ESI-MS) were recorded on a QTOF Micro YA 263 mass spectrometer in the positive ion mode. Fluorescence spectra were obtained with a fluorescence spectrometer (Edinburgh Instruments, U.K.). The fluorescence imaging was obtained with a confocal instrument (TCS SPE, Leica, Germany).

Synthesis of Arg-Cy. First, 0.1 g of tricarbochlorocyanine dye (Cy.7.Cl) (0.366 mmol) was dissolved in 10 mL of dimethylformamide (DMF), and 0.233 g of L-arginine was dissolved in 2 mL of water. After thoroughly mixing the two solutions, the mixture was slowly heated to 70 °C under an argon atmosphere for 5 h in a 50 mL round-bottom flask. Then, the solvent was removed by evaporation, and the residue was subjected to silica gel chromatography and eluted with ethyl acetate/methanol (5:1 v/v), affording Arg-Cy as a blue solid. The ^{1}H NMR and ^{13}C NMR spectra of Arg-Cy are presented in Figures S1 and S2 of the Supporting Information, respectively. ^{1}H NMR (400 MHz, DMSO-d_6): δ 9.45 (s, 1H), 8.55 (s, 1H), 8.04 (s, 1H), 7.83 (d, J = 12.0 Hz, 2H), 7.57 (s, 1H), 7.44 (s, 2H), 7.25 (s, 2H), 7.01−7.08 (m, 4H), 5.74 (d, J = 12.0 Hz, 2H), 4.19 (s, 1H), 3.95(s, 4H), 3.11 (s, 2H), 2.51 (s, 2H), 2.43 (s, 2H), 1.91−2.06 (m, 2H), 1.72 (s, 2H), 1.35−1.47 (m, 14H), 1.05−1.09 (m, 6H). ^{13}C NMR (100 MHz, DMSO-d_6): δ 174.1, 167.7, 166.7, 158.2, 142.8, 140.5, 138.1, 128.5, 122.6, 120.6, 109.1, 94.5, 62.7, 47.5, 37.6, 28.6, 28.0, 25.6, 25.1, 21.8, 11.7. MS: calcd 649.4230, found 649.4203 (Supporting Information Figure S3).

Cell Culture and Preparation of Cell Disruption Liquids. HepG2 cells were cultured with RPMI-1640 medium (Gibco, Carlsbad, CA, U.S.A.) supplemented with 10% fetal bovine serum (FBS) and 1% antibiotics (100 U/mL penicillin and 100 mg/mL streptomycin) at 37 °C under a humidified atmosphere of 95% air and 5% CO_2. Cells in the logarithmic phase of growth were used throughout the cell experiments. To prepare the cell disruption liquids, HepG2 cells were seeded in 60 mm circular Petri dishes at a density of 2 × 10^4 cells/mL with 4 mL per dish and incubated for 24 h. Then, the cells were stained with Arg-Cy for 15 min. After washing twice with PBS, the cells were harvested and broken in PBS buffer for 10 min using a cell disruptor (VC130PB, Sonics, U.S.A.) at 0−4 °C. After equally distributing the cell disruption liquids into different centrifuge tubes, DHA was added to the tubes and coincubated for different times, followed by centrifuging at 3000 rpm for 10 min at 4 °C. The supernatant was collected, and its fluorescence was measured. The process for preparing the cell disruption liquids is shown in Figure S4 of the Supporting Information.

Fluorescence Imaging in Living Cells. HepG2 cells were grown on glass-bottom culture dishes. After treatment with AA,

DOI: 10.1021/acs.analchem.5b00820
Anal. Chem. 2015, 87, 7092−7097

the cells were further incubated with 50 μM Arg-Cy in FBS-free 1640 medium at 37 °C for 15 min and then washed three times with PBS buffer (pH 7.4). Then, the cells were imaged immediately using a confocal microscope with an objective lens (×40). Excitation of probe-loaded cells at 635 nm was performed using an argon laser, and the emitted light was collected with an META detector between 650 and 750 nm.

Cytotoxicity Assay. The cytotoxicity of Arg-Cy to HepG2 cells was evaluated by MTT assay according to our previous report.[17] In brief, cells were seeded in 96-well flat-bottom microtiter plates at a density of 20 000 cells/mL with 100 μL per well, incubated for 24 h, and then exposed to different concentrations (1−200 μM) of Arg-Cy at 37 °C for 24 h. Then, the culture media were discarded and 20 μL of MTT solution (5 mg/mL) was added to each well, followed by incubation at 37 °C for 4 h. The supernatant was discarded, and 100 μL of DMSO was added to each well to dissolve the crystals. After shaking for 10 min, the absorbance of the solution was measured at 490 nm using a microtiter plate reader. The cell viability rate (VR) was calculated according to the following formula: VR = A490 (sample)/A490 (control) × 100%. The cell survival rate from the control group was considered to be 100%. At least three replicates were performed.

RESULTS AND DISCUSSION

Spectroscopic Properties of Arg-Cy. The excitation and emission spectra of Arg-Cy are located at 680 and 749 nm, respectively, as shown in Figure 1. The data show that Arg-Cy has a large Stokes shift of approximately 69 nm, which is a desired property in the probe design because it can improve the detection sensitivity.

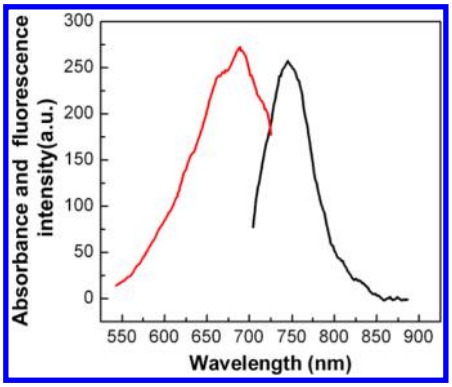

Figure 1. Excitation and emission spectra of Arg-Cy, $\lambda_{ex}/\lambda_{em}$ = 680/749 nm.

Fluorescence Response of Arg-Cy toward the Metabolite of DHA in the Cell Disruption Liquids. In most cancer cells, AA enters into cells in the form of DHA.[18] To better simulate the microenvironment of the cell, we chose DHA instead of AA to detect the response of Arg-Cy toward the metabolites of Vc in the simulative biological system. First, the fluorescence changes before and after adding DHA to the solution of Arg-Cy in 0.1 M sodium phosphate buffer (pH 7.0) were recorded. Figure 2A indicates that the probe does not respond to DHA. Second, we selected the cell disruption liquids (see cell culture and preparation of cell disruption liquids in the Experimental Section) of HepG2 cells to test the response of Arg-Cy to the metabolic products of DHA. As shown in Figure 2A, when only the probe was added to the

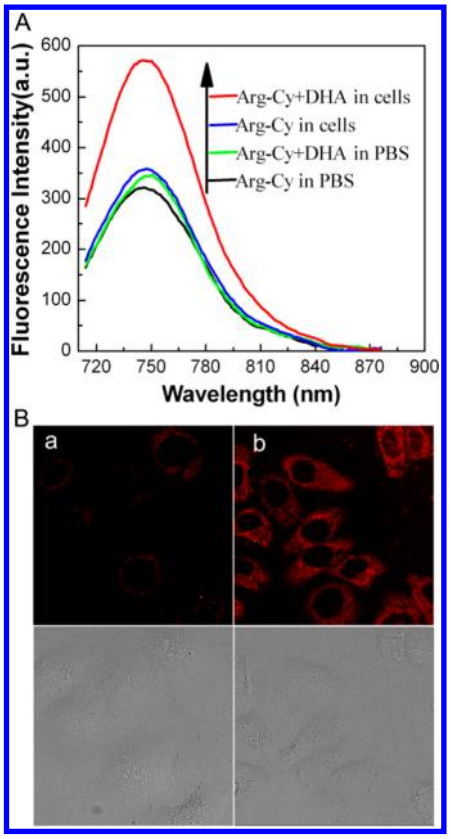

Figure 2. (A) Fluorescence response to the metabolite of DHA. 10 μM DHA was added to 0.1 M PBS (pH 7.0) at 37 °C and to the supernatant of cell disruption liquids, respectively, with and without 50 μM Arg-Cy. (B) Fluorescence images: (a) HepG2 cells were incubated with 50 μM Arg-Cy for 15 min at 37 °C; (b) HepG2 cells were incubated with 10 μM DHA for 15 min, followed by the addition of 50 μM Arg-Cy for 15 min. $\lambda_{ex}/\lambda_{em}$ = 680/749 nm.

cells, in the supernatant of the cell disruption liquids, Arg-Cy exhibits negligible fluorescence; however, after adding 10 μM DHA to these cell disruption liquids for 15 min, the fluorescence intensity clearly increased. In addition, a preliminary imaging analysis was performed. Figure 2B shows that only the probe-loaded cells treated with DHA emit bright red fluorescence. These results indicate that Arg-Cy can respond to the metabolites of DHA.

ESI-MS Analysis of the Reaction Product of Arg-Cy with the Metabolite of DHA. Pischetsrieder[11] found that, when heated in aqueous solution, AA is easily oxidized into DHA and that the lactone ring of DHA immediately opens to produce 2,3-diketogulonic acid (DKG). Then, DKG is decarboxylated to L-xylosone. Later, several studies identified 3-deoxythreosone and oxalate as the major degradation products in the nonoxidative degradation process of DHA, and in the oxidative degradation pathway, DHA predominantly produces L-threosone and L-xylosone.[12,13,19−23] On the basis of the above reports, the reaction product of Arg-Cy with the metabolites of DHA was discovered from acquired high-resolution mass spectrum (HRMS). As shown in Figure 3a, only one major peak at m/z 761.4 was obtained, which corresponds to the product (calculated m/z: 761.4385 [M^+]) of the reaction of Arg-Cy with L-xylosone. The result implies that the contents of other metabolites containing adjacent diketone may be too low to be detected. To further prove Arg-Cy can label L-xylosone, we synthesized the L-xylosone and the reaction

DOI: 10.1021/acs.analchem.5b00820
Anal. Chem. 2015, 87, 7092−7097

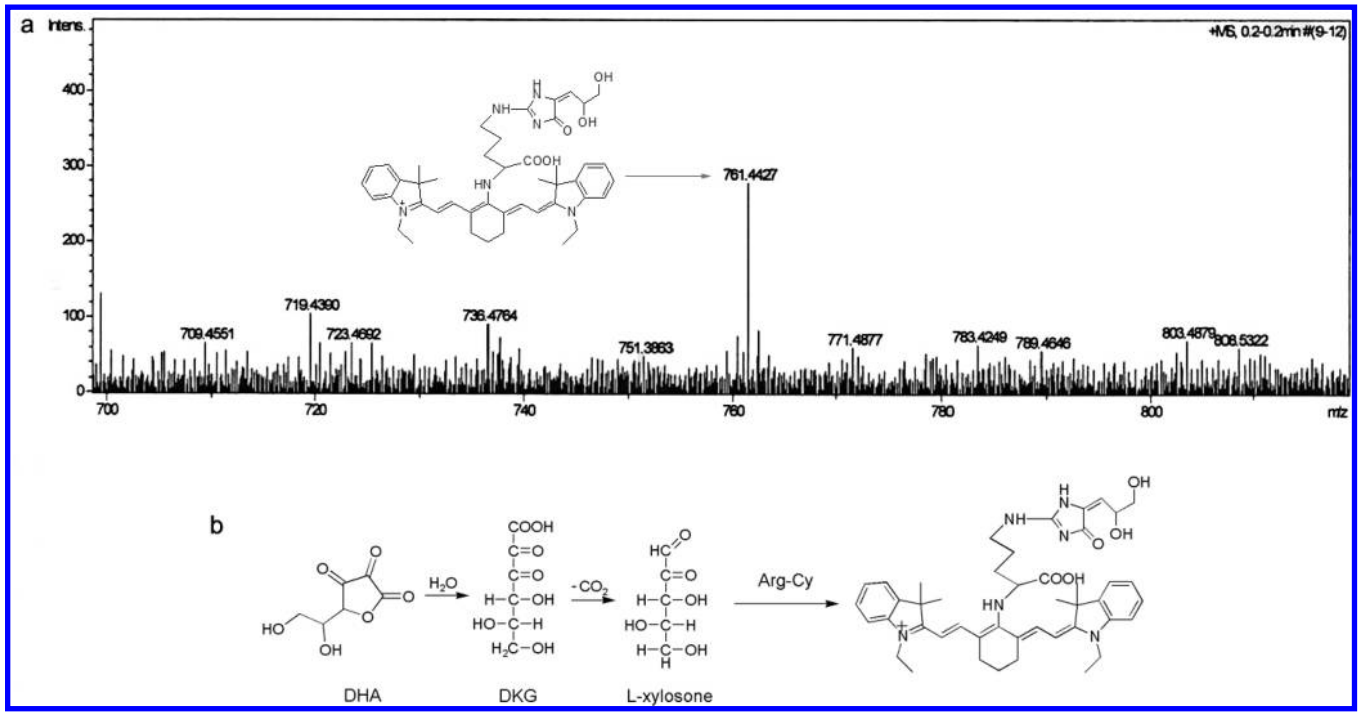

Figure 3. (a) ESI-MS spectrum showing the reaction of Arg-Cy with L-xylosone. HepG2 cells were incubated with 10 μM DHA for 15 min, followed by the addition of 50 μM Arg-Cy for 15 min at 37 °C. After washing twice with PBS, the cells were harvested and broken in FBS-free RPMI-1640 medium with cell disruptor for 10 min at 0−4 °C. After centrifuging at 4 °C, the supernatant was collected and measured using mass spectrometry. (b) The reaction process of Arg-Cy with L-xylosone.

product of Arg-Cy with L-xylosone was detected by ESI-MS (Supporting Information Figure S7). The hypothesized process for the reaction of Arg-Cy with L-xylosone is shown in Figure 3b.[11,19]

Spectroscopic Response of Arg-Cy to L-Xylosone. The conditions for the responses of Arg-Cy to L-xylosone were first optimized in the supernatant of the cell disruption liquids, as shown in Supporting Information Figure S8. Supporting Information Figure S8a shows that the fluorescence intensities gradually increase with increasing concentrations of Arg-Cy and reach a plateau at 50 μM Arg-Cy. Supporting Information Figure S8b indicates that the strongest fluorescence intensity is obtained at a reaction time approximately 90 min. Therefore, in the following experiments, the cells were incubated with 50 μM Arg-Cy for 15 min and were disrupted by ultrasonication; then, different concentrations of DHA were added to the disruption liquids for 90 min. The obtained supernatants were used to test the fluorescence response of Arg-Cy to L-xylosone produced by DHA. As shown in Figure 4, a gradual increase in the fluorescence intensity was observed when adding the supernatant of cells treated with different concentrations of DHA under the optimal conditions, and there is a good linearity between the fluorescence intensities and DHA concentrations in the range 0−10 μM (inset). The regression equation is F = 323.09 + 31.25[DHA] (μM), with a linear coefficient of 0.9969.

Reaction Selectivity of Arg-Cy. To determine the reaction selectivity of Arg-Cy, various potential interfering species, such as reactive oxygen species (H_2O_2, ·OH, and $O_2^{-\bullet}$), *t*-BuOOH, NaClO, dopamine, NO, glucose, lactose, maltose, and amino acids (cystine, Cys, Lys, and Trp), were examined in parallel under the same conditions (Figure 5). In addition, the interference from metal ions is shown in Supporting Information Figure S9a. Arg-Cy exhibits an obvious increase in fluorescence intensity upon reaction with the

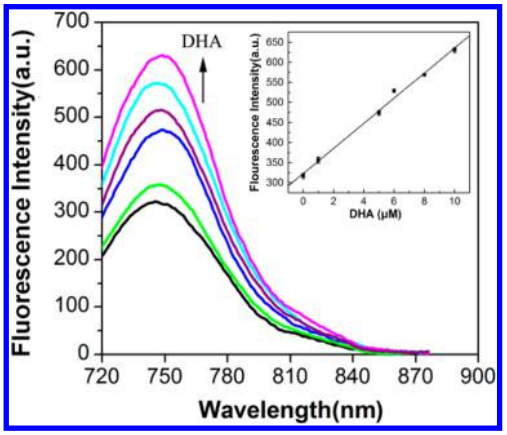

Figure 4. Fluorescence responses of 50 μM Arg-Cy to L-xylosone at varied concentrations of DHA (0, 1, 5, 6, 8, 10 μM). Inset: a linear correlation between emission intensities and concentrations of DHA. $\lambda_{ex}/\lambda_{em}$ = 680/749 nm.

metabolite of DHA, whereas the responses toward other interfering species are negligible. The concentrations of the selected interfering species were considerably higher than the intracellular concentrations. Notably, when GSH was added at a millimolar concentration level to the cell disruption liquids followed by the addition of DHA, the fluorescence change was not obvious (Supporting Information Figure S9b). This result demonstrates that the metabolism of DHA is inhibited under a reducing environment. Furthermore, there are many endogenous α-oxoaldehydes like glyoxal exist in vivo and can reacted with Arg,[24] so the selectivity experiment to glyoxal was carried out. The result indicates that Arg-Cy cannot react with glyoxal (Supporting Information Figure S9c), which should be due to a strong hydration of glyoxal.

DOI: 10.1021/acs.analchem.5b00820
Anal. Chem. 2015, 87, 7092−7097

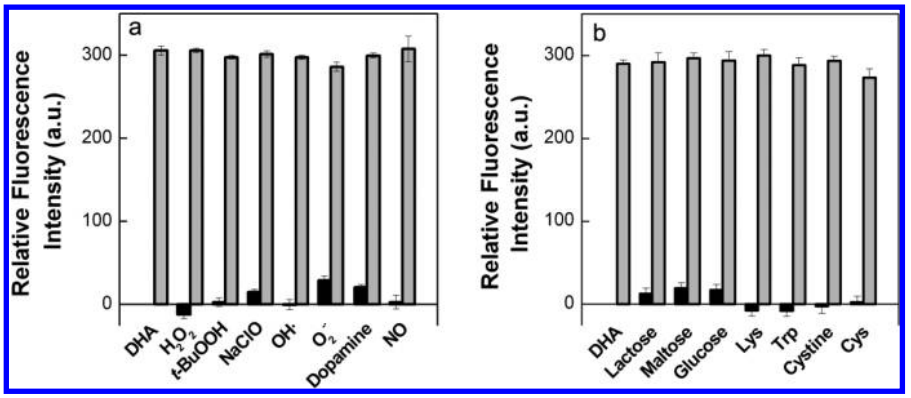

Figure 5. (a) Fluorescence responses of 50 μM Arg-Cy to ROS (black bars) and ROS plus 10 μM DHA (gray bars): H_2O_2 (0.1 mM), *t*-BuOOH (30 μM), NaClO (24 μM), ·OH (24 μM), $O_2^{-\bullet}$ (300 nM), dopamine (0.3 mM), NO (20 μM). (b) Fluorescence responses of 50 μM Arg-Cy to sugars/amino acids (black bars) and sugars/amino acids plus 10 μM DHA (gray bars): lactose, maltose, glucose (0.5 mM), Lys, Trp, cystine, Cys (0.1 mM). $\lambda_{ex}/\lambda_{em}$ = 680/749 nm.

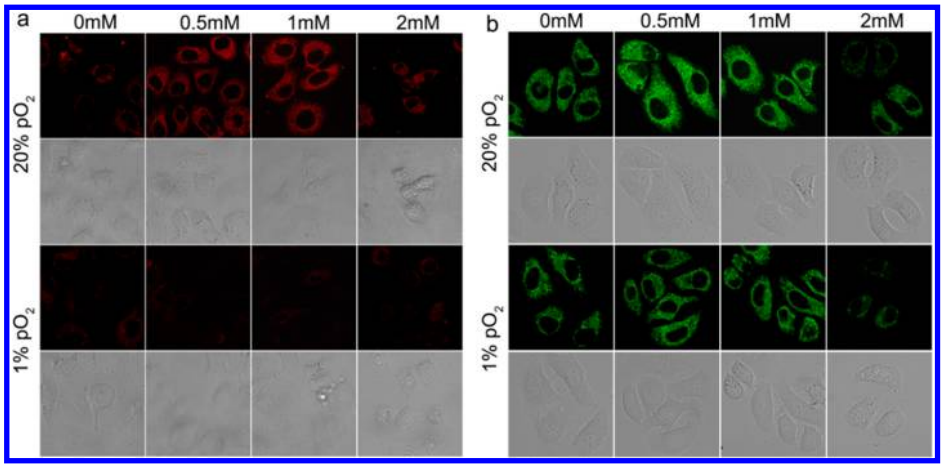

Figure 6. Fluorescence images of the changes in the levels of L-xylosone and H_2O_2 in HepG2 cells. HepG2 cells were exposed to different concentrations of AA (0−2 mM) for 6 h at 37 °C under normoxic conditions (20% pO_2) and hypoxic conditions (1% pO_2); then, the cells were incubated with 50 μM Arg-Cy for 15 min, and the fluorescence was imaged using a confocal microscope with 635 nm excitation and 650−750 nm collection (a), or the cells were incubated with 10 μM H_2O_2 probe for 15 min and detected using a confocal microscope with 532 nm excitation and 600−700 nm collection (b).

Fluorescence Imaging of L-Xylosone in Living Cells. Several studies have shown that vitamin C can kill cancer cells.[25,26] However, the mechanism for the antitumor action of vitamin C is highly controversial. In this study, we simulated the tumor microenvironment to observe the mechanism of AA inducing HepG2 cell death. First, HepG2 cells were exposed to 0−2 mM AA at 37 °C for 6 h under normoxic conditions (20% pO_2) and hypoxic conditions (1% pO_2); then, the cells were incubated with 50 μM Arg-Cy for 15 min. As shown in Figure 6a, HepG2 cells treated with 0−1 mM AA under normoxic conditions showed an increase in fluorescence in a concentration-dependent manner; however, with 2 mM AA, the cells began to die (the cells shrank and became round; see the bright field image in Figure 6a) accompanied by a decrease in fluorescence. Notably, the cells under hypoxic conditions exhibited negligible intracellular background fluorescence. An additional experiment was performed using 1 mM AA for different times (0−9 h), and as shown in Supporting Information Figure S10, the obtained results are identical. These results indicate that AA degrades to form L-xylosone under normoxic conditions but not under hypoxic conditions. To further demonstrate that the production of L-xylosone is related to an intracellular redox environment, a H_2O_2 probe[27] was used to detect the ROS level (the synthesis and characterization of H_2O_2 probe is described in the Supporting Information). HepG2 cells were exposed to different concentrations of AA (0−2 mM) for up to 6 h under normoxic conditions or hypoxic conditions, and then the cells were incubated with 10 μM of the H_2O_2 probe for 15 min. As shown in Figure 6b, the cells treated with 0.5−1 mM AA exhibited significantly higher levels of H_2O_2 under normoxia, and the fluorescence disappeared as the cell died. This result confirms that, under normoxic conditions, AA indeed exhibits a pro-oxidant function by inducing an increase in the production of reactive oxygen species (ROS) that triggers cell death, which is consistent with previous studies.[5,28] In contrast, under hypoxic conditions, the cells exhibit negligible changes in fluorescence intensity before cell death, demonstrating that no oxidative stress occurs in the process of AA antihepatoma. On the basis of the two experiments above, we conclude that AA can be metabolized to L-xylosone under a normal oxygen environment and induce oxidative stress which leads to cell death; however, under hypoxic conditions, AA cannot produce L-xylosone and does not induce oxidative stress until cell death. We hypothesize that the cell death induced by AA under hypoxic conditions may be attributed to the reductive stress. Thus, this

DOI: 10.1021/acs.analchem.5b00820
Anal. Chem. 2015, 87, 7092−7097

probe may help to clarify the mechanism for the antitumor activity of vitamin C in a tumor microenvironment.

To evaluate the potential toxicity of Arg-Cy to cells, an MTT assay was performed, as shown in Supporting Information Figure S11. The result indicates that the cytotoxicity of Arg-Cy is low under the employed experimental conditions, indicating that the probe possesses low cytotoxicity and good biocompatibility. Finally, a photobleaching test was performed through time-sequential scanning of probe-loaded HepG2 cells. After 300 s of continuous excitation with 635 nm, no obvious indications of photobleaching were observed (Supporting Information, Figure S12). These results demonstrate that the probe can be targeted into living cells with low cytotoxicity and minimal photobleaching.

CONCLUSIONS

In summary, we designed and synthesized a near-infrared fluorescent probe, Arg-Cy. This probe, for the first time, enables the real-time visualization of the metabolic products of vitamin C in living cells. The developed probe provides a tool for the rapid detection and imaging of L-xylosone in vitro and in living cells. Furthermore, the probe can also be used to distinguish the different metabolic states of vitamin C in HepG2 cells under normoxic conditions and hypoxic conditions, and we found that vitamin C can be metabolized to L-xylosone only under normoxic conditions, not under hypoxic conditions. Therefore, we propose that reductive stress may be the key factor for HepG2 cell death induced by vitamin C under hypoxic conditions. Further studies on the reductive stress induced by vitamin C in the tumor microenvironment are currently underway.

ASSOCIATED CONTENT

Supporting Information

Additional information as noted in text. The Supporting Information is available free of charge on the ACS Publications website at DOI: 10.1021/acs.analchem.5b00820.

AUTHOR INFORMATION

Corresponding Authors

*E-mail: tangb@sdnu.edu.cn.
*E-mail: xukehua@sdnu.edu.cn.

Notes

The authors declare no competing financial interest.

ACKNOWLEDGMENTS

This work was supported by the 973 Program (2013CB933800) and National Natural Science Foundation of China (21227005, 21390411, 91313302, 21275092).

REFERENCES

(1) Montecinos, V.; Guzmán, P.; Barra, V.; Villagrán, M.; Muñoz-Montesino, C.; Sotomayor, K.; Escobar, E.; Godoy, A.; Mardones, L.; Sotomayor, P.; Guzmán, C.; Vásquez, O.; Gallardo, V.; van Zundert, B.; Bono, M. R.; Oñate, S. A.; Bustamante, M.; Cárcamo, J. G.; Rivas, C. I.; Vera, J. C. *J. Biol. Chem.* **2007**, *282*, 15506−15515.
(2) Mamede, A. C.; Pires, A. S.; Abrantes, A. M.; Tavares, S. D.; Gonçalves, A. C.; Casalta-Lopes, J. E.; Sarmento-Ribeiro, A. B.; Maia, J. M.; Botelho, M. F. *Nutr. Cancer* **2012**, *64*, 1049−1057.
(3) Mamede, A. C.; Tavares, S. D.; Abrantes, A. M.; Trindade, J.; Maia, J. M.; Botelho, M. F. *Nutr. Cancer* **2011**, *63*, 479−494.
(4) Toohey, J. I. *Cancer Lett.* **2008**, *263*, 164−169.
(5) Gonçalves, A. C.; Alves, V.; Silva, T.; Carvalho, C.; Oliveira, C. R.; Sarmento-Ribeiro, A. B. *Toxicol. In Vitro* **2013**, *27*, 1542−1549.
(6) Song, J. H.; Shin, S. H.; Wang, W.; Ross, G. M. *Exp. Neurol.* **2001**, *169*, 425−437.
(7) Heaney, M. L.; Gardner, J. R.; Karasavvas, N.; Golde, D. W.; Scheinberg, D. A.; Smith, E. A.; O'Connor, O. A. *Cancer Res.* **2008**, *68*, 8031−8038.
(8) Verrax, J.; Calderon, P. B. *Biochem. Pharmacol.* **2008**, *l76*, 1644−1652.
(9) Denko, N. C. *Nat. Rev. Cancer* **2008**, *8*, 705−713.
(10) Harris, A. L. *Nat. Rev. Cancer* **2002**, *2*, 38−47.
(11) Pischetsrieder, M. *J. Agric. Food Chem.* **1996**, *44*, 2081−2085.
(12) Simpson, G. L.; Ortwerth, B. J. *Biochim. Biophys. Acta* **2000**, *1501*, 12−24.
(13) Nemet, I.; Monnier, V. M. *J. Biol. Chem.* **2011**, *286*, 37128−37136.
(14) Sasaki, E.; Kojima, H.; Nishimatsu, H.; Urano, Y.; Kikuchi, K.; Hirata, Y.; Nagano, T. *J. Am. Chem. Soc.* **2005**, *127*, 3684−3685.
(15) Yin, J.; Kwon, Y.; Kim, D.; Lee, D.; Kim, G.; Hu, Y.; Ryu, J. H.; Yoon, J. *J. Am. Chem. Soc.* **2014**, *136*, 5351−5358.
(16) Xu, K.; Qiang, M.; Gao, W.; Su, R.; Li, N.; Gao, Y.; Xie, Y.; Kong, F.; Tang, B. *Chem. Sci.* **2013**, *4*, 1079−1086.
(17) Xu, K.; Wang, F.; Pan, X.; Liu, R.; Ma, J.; Kong, F.; Tang, B. *Chem. Commun.* **2013**, *49*, 2554−2556.
(18) Agus, D. B.; Vera, J. C.; Golde, D. W. *Cancer Res.* **1999**, *59*, 4555−4558.
(19) Reihl, O.; Lederer, M. O.; Schwack, W. *Carbohydr. Res.* **2004**, *339*, 483−491.
(20) Nishikawa, Y.; Toyoshima, Y.; Kurata, T. *Biosci., Biotechnol., Biochem.* **2001**, *65*, 1707−1712.
(21) May, J. M. *Front. Biosci.* **1998**, *3*, 1−10.
(22) Banhegyi, G.; Braun, L.; Csala, M.; Puskas, F.; Mandl, J. *Free Radical Biol. Med.* **1997**, *23*, 793−803.
(23) Deutsch, J. C. *J. Chromatogr. A* **2000**, *881*, 299−307.
(24) Sibbersen, C.; Palmfeldt, J.; Hansen, J.; Gregersen, N.; Jørgensen, K. A.; Johannsen, M. *Chem. Commun.* **2013**, *49*, 4012−4014.
(25) Du, J.; Martin, S. M.; Levine, M.; Wagner, B. A.; Buettner, G. R.; Wang, S. H.; Taghiyev, A. F.; Du, C.; Knudson, C. M.; Cullen, J. J. *Clin. Cancer Res.* **2010**, *16*, 509−520.
(26) Valenti, M. T.; Zanatta, M.; Donatelli, L.; Viviano, G.; Cavallini, C.; Scupoli, M. T.; Dalle Carbonare, L. *Anticancer Res.* **2014**, *34*, 1617−1627.
(27) Karton-Lifshin, N.; Segal, E.; Omer, L.; Portnoy, M.; Satchi-Fainaro, R.; Shabat, D. *J. Am. Chem. Soc.* **2011**, *133*, 10960−10965.
(28) Rawal, M.; Schroeder, S. R.; Wagner, B. A.; Cushing, C. M.; Welsh, J. L.; Button, A. M.; Du, J.; Sibenaller, Z. A.; Buettner, G. R.; Cullen, J. J. *Cancer Res.* **2013**, *73*, 5232−5241.

DOI: 10.1021/acs.analchem.5b00820
Anal. Chem. 2015, 87, 7092−7097